AIAA JOURNAL
Vol. 31, No. 8, August 1993

Delamination in Cross-Ply Laminated Composite Subjected to Low-Velocity Impact

H. Razi*
Boeing Commercial Airplane Group, Seattle, Washington 98124
and
A. S. Kobayashi†
University of Washington, Seattle, Washington 98122

Delamination due to low-velocity impact of simply supported graphite/epoxy cross-ply laminate beams and plates was investigated. Both quasistatic and low-velocity impact testing were carried out in this study. For each loading condition, finite element analysis and experiments were performed to study damage growth and distributions. The mode II energy release rate for dynamic crack arrest G_{IIa} was 75% less than the onset of crack propagation G_{IIC}. A quasistatic three-dimensional finite element analysis coupled with a $G_{II} \geq G_{IIC}$ criterion was used for the onset of delamination propagation, and $G_{II} \leq G_{IIa}$ criterion was used to arrest the propagating crack and to estimate the delamination area. Delamination area determined by this method correlated well with the test results.

Introduction

STRUCTURES made of composite parts are susceptible to damage which may manifest itself in fiber breakage, matrix cracking, and delamination during fabrication or service. The main focus of this paper is to investigate criteria for delamination growth and arrest.

Prediction methodologies of delamination damage area in composites due to low-velocity impact have been proposed by several authors. Graves and Kantz[1] used the maximum shear-stress failure criterion to estimate the damage area; however, this criterion does not predict the type and distribution of damage through the thickness. The model of Clark[2] provides only qualitative predication of the delamination size. The models of Bostaph and Elber,[3] Grady and Sun,[4] and Grady and Depaola[5] provide an estimate of the delamination growth but require prior knowledge of the number and location of delaminations. The model of Gosse and Mori[6] and Gosse et al.[7] provides the location and shapes but not the size of delamination. Chang et al.[8] used the dynamic finite element method coupled with failure analysis to predict threshold of impact damage and initiation of delamination. Finn[9] used von Mises failure theory to predict damage initiation stress and strain energy density to predict delamination size.

The purpose of this paper is to establish a criteria that control delamination propagation and arrest in a composite beam when subjected to static and dynamic loadings. These criteria are then used in conjunction with finite element analysis to estimate the delamination area in the composite plates.

Quasistatic Testing

Beam Specimens—Three-Point Bending

A total of 16 beam specimens with 2.54×6.35 cm (1×2.5 in.) were used to study damage initiation and propagation under quasistatic three-point bend loading. These specimens were fabricated using Hitex 46/F650 graphite/bismalemide unidirectional tape with $[(0)_4/(90)_4]_s$ and $[(90)_4/(0)_4]_s$ layups. The diameter of the point load was 0.635 cm (0.25 in.). The specimens were simply supported at both ends. At each load increment, the specimen was scanned with a microscope of magnification 20 to check for damage; then the displacement was increased until delamination was initiated and propagated. The delamination length was then measured by a microscope of magnification 100.

Finite Element Analysis

Arrest Strain Energy Release Rate

Figures 1 and 2 show typical damage distribution in $[(0)_4/(90)_4]_s$ and $[(90)_4/(0)_4]_s$ layups. A two-dimensional, nonlinear finite element analysis was performed using the finite element mesh shown in Fig. 3. Because of symmetry in the loading and the geometry, only one-half of the specimen was modeled. The model contains 170 isoparametric quadrilateral plane strain elements and 440 degrees of freedom.

Figures 4 and 5 show the plot of load vs load-line displacement of $[(0)_4/(90)_4]_s$ and $[(90)_4/(0)_4]_s$ laminated beams, respectively. The load history was divided into five increments and static finite element analysis coupled with the failure crite-

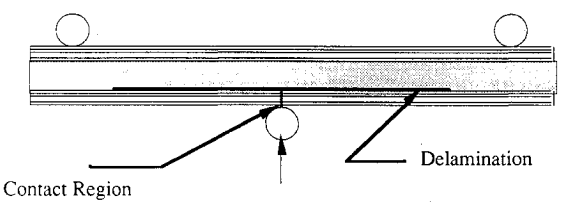

Fig. 1 Damage distribution in $[(0)_4/(90)_4]_s$ laminate for static loading.

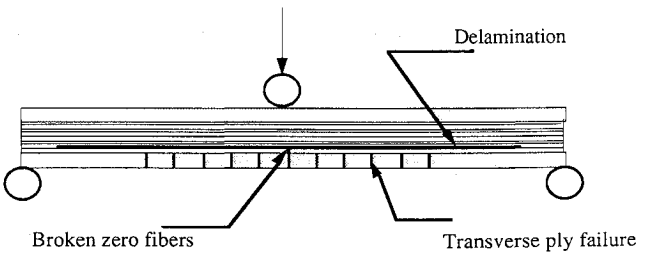

Fig. 2 Damage distribution in $[(90)_4/(0)_4]_s$ laminate.

Received Jan. 29, 1992; presented as Paper 92-2555 at the AIAA/ASME/ASCE/AHS/ASC 33rd Structures, Structural Dynamics, and Materials Conference, Dallas, TX, April 13-15, 1992; revision received Nov. 23, 1992; accepted for publication Nov. 29, 1992.

*Specialist Engineer, Stress Methods.
†Professor, Department of Mechanical Engineering.

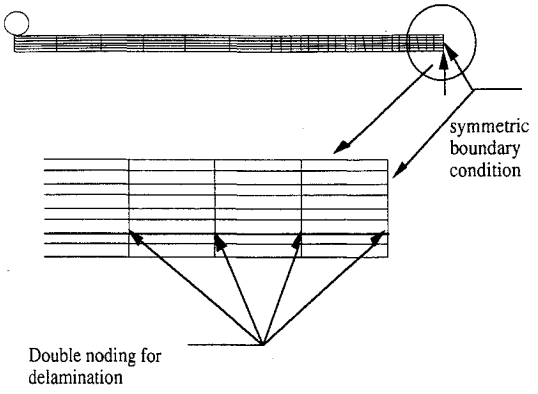

Fig. 3 Finite element mesh for beam specimen.

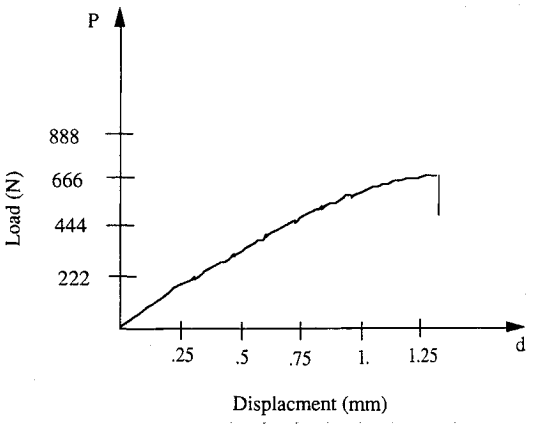

Fig. 4 Load vs load-line displacement for $[(90)_4/(0)_4]_s$ laminate.

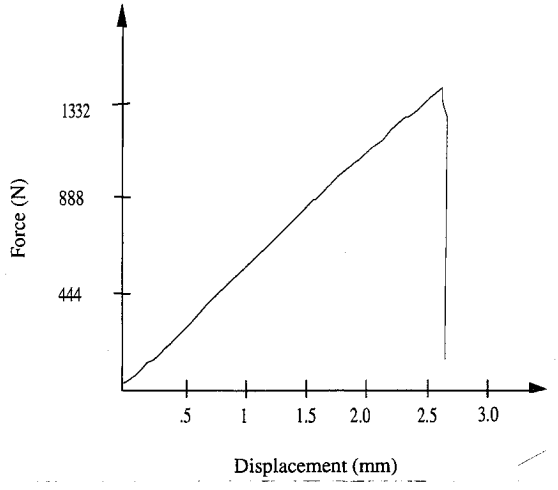

Fig. 5 Load vs load-line displacement for $[(0)_4/(90)_4]_s$ laminate.

rion based on the maximum principal stress was used to analyze increment of crack extension. The stiffness of those elements, in which the maximum principal stresses exceeded the tensile strength in the principal direction, were set to zero in the next increment. This incremental analysis was carried out to the maximum displacement recorded in the test. At this maximum displacement, the nodes at the delamination area (Fig. 3) were released and replaced with the gap elements. Energy release rate was calculated using the crack closure integral methods[10] at each nodal advanced.

Results and Discussion

Figures 6 and 7 show the plot of G_{II} vs crack length. The arrest strain-energy release rate G_{IIa} is the same for both laminates (i.e., 104 J/m^2). The value of G_{IIa} was used as a criterion to estimate the delamination area in the plate specimen under quasistatic loading.

Plate Specimens—Simply Supported with a Central Load

Four panels of 7.62×7.62 cm (3×3 in.) and $[(0)_4/(90)_4]_s$ layup were used to study the damage distribution in the composite panels under quasistatic loading. These panels are fabricated using Hitex 46/F650 graphite/bismalemide unidirectional tape. These specimens were simply supported at all edges. A 0.635-cm (0.25-in.) point-nose diameter was used to apply displacement loading at the center of the plate. The test was continued until the load reached the maximum load recorded in the drop-weight impact testing which is discussed in the following section. Specimens were then ultrasonic C-scanned and cross sectioned for detailed study of the damage

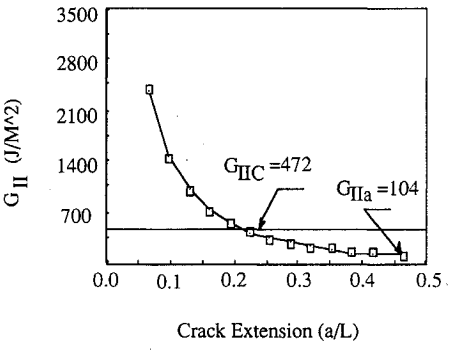

Fig. 6 Effect of crack length on G_{II} of $[(0)_4/(90)_4]_s$ laminate.

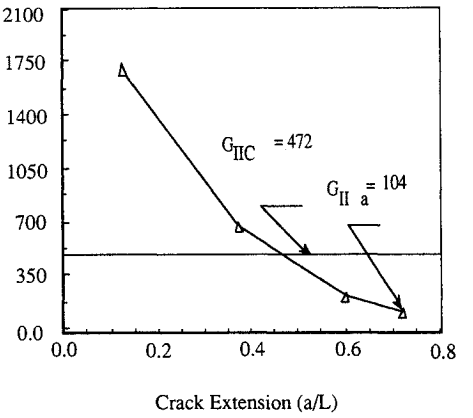

Fig. 7 Mode II strain energy release rate vs crack extension for $[(90)_4/(0)_4]_s$ laminate.

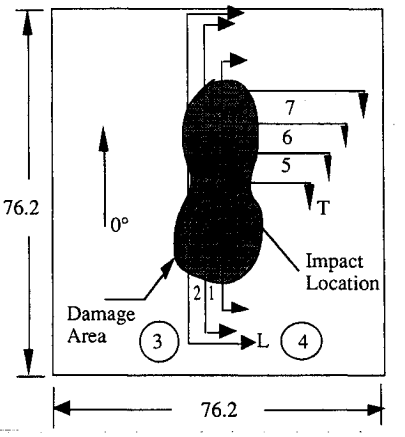

Fig. 8 Relative position of cross section from impact location.

distribution through the thickness. This damage due to quasi-static loading was then compared with the damage caused by the drop-weight loading.

Sectioning and Microscopy of Damaged Specimens

Figure 8 depicts a C-scan picture of the specimen and the relative position of the cross sections used in subsequent microscopic study. Figure 9 shows the sizes and locations of the delaminations for each cross section. Through-the-thickness damage was dominated by delamination and 45-deg cone-type shear failure.

Finite Element Analysis

A three-dimensional linear elastic finite element model coupled with a fracture criterion was used to estimate the damage area. The final finite element model contained 1600 eight-noded elements and 7938 degrees of freedom (Fig. 10a). The delamination area was modeled with coincident nodes and gap elements were used between these nodes to prevent overlapping of the coincident surfaces. Details in the vicinity of delamination front are shown in Fig. 10b. Because of symmetries in the geometry and loading condition, only one-quarter of the panel was modeled.

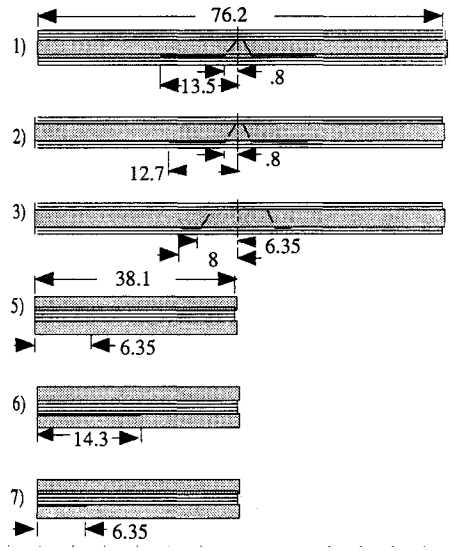

Fig. 9 Typical damage distribution in cross section shown in Fig. 8.

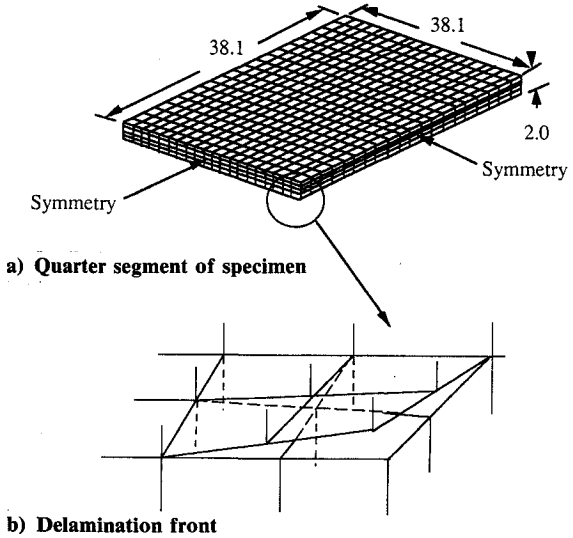

Fig. 10 Finite element model of composite panel.

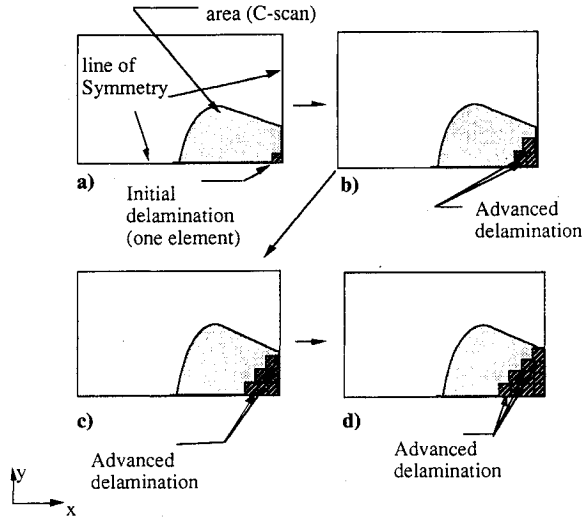

Fig. 11 Variation in delamination shape and size in quarter segment of plate specimen.

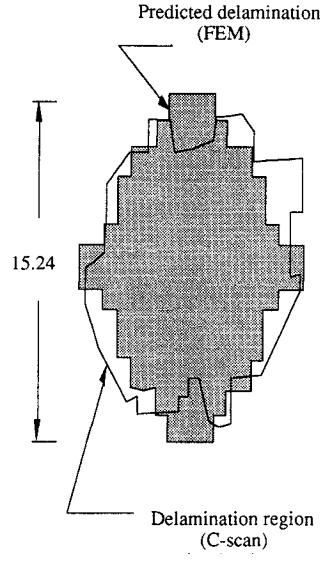

Fig. 12 Comparison of damage areas between the C-scan and the finite element analysis.

Incremental quasistatic finite element analysis was used and strain-energy release rate was calculated by the change of stored elastic energy per unit extension of the delamination. At the maximum displacement (i.e., recorded in the quasistatic test), it was assumed that the delamination was equal to the size of one element (Fig. 11a). Then the strain-energy release rate was calculated in the x and y directions as follows. In the first computation, the delamination was assumed to propagate one element in the x or y direction (Fig. 11b). The strain energy required to extend the crack one element in the x or y direction is $G_{II}\,dA$. The strain-energy release rate was compared with the critical strain-energy release rate of the material G_{IIC} to determine the onset of delamination extension. The criteria of delamination propagation was $G_{II} \geq G_{IIC}$. In the next computation, the input displacement was assumed constant, but the model was modified such that the delamination was extended to the next element by opening the nodes and inserting the gap elements beween them. The same method, which was employed in the preceding computation, was used in this load step but the delamination was extended (Fig. 14c) when $G_{II} \geq G_{IIa}$. This procedure was repeated until $G_{II} < G_{IIa}$ for all elements in the delamination region. Figure 14 shows the steps for determining the delamination shape and size. The material proper-

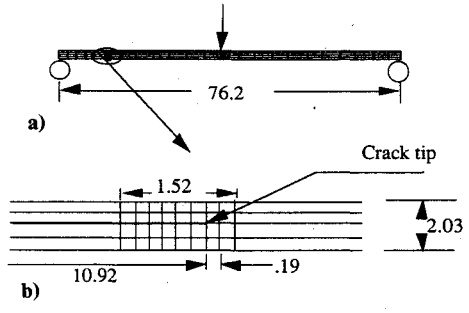

Fig. 13 Finite element model of end-notch-flexure specimen.

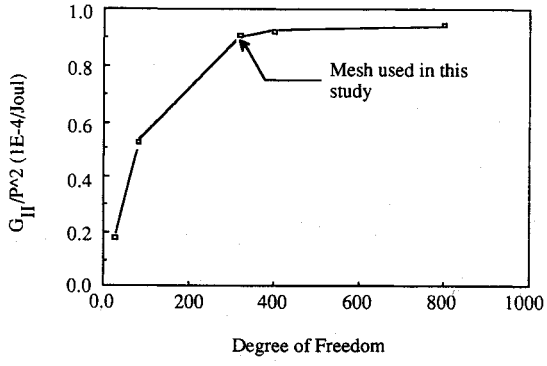

Fig. 14 Effect of finite element mesh size on G_{II} computation.

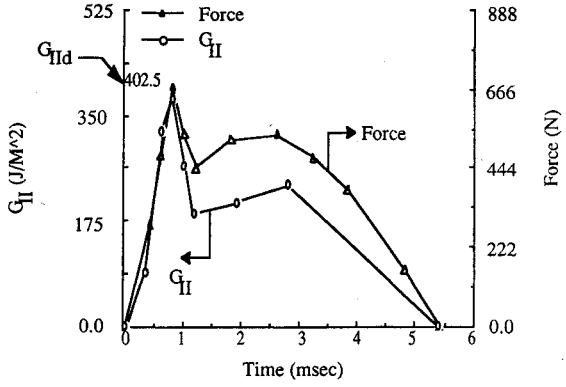

Fig. 15 Load and strain energy release rate history due to low-velocity impact.

ties used in the finite element analysis are summarized in Table 1. These properties were determined experimentally under this research project.[11] The out-of-plane mechanical properties of the laminas were taken to be the same as the transverse property.

The through-the-thickness damage of an impacted specimen was a 45-deg cone-type shear failure in addition to the delamination between 0- and 90-deg plies. Several finite element models, which include this type of shear failure, were analyzed where this failure was found to be insignificant in the overall estimation of G_{II}. Therefore, the cone-type shear failure was not included in subsequent finite element analysis to simplify the modeling.

Results

Figure 12 shows excellent agreement between predicted damage from the finite element modeling with the experimental results.

Table 1 Summary of mechanical properties

E_{11}	Tension	177.8, GPa
E_{22}	Tension	12.4, GPa
G_{12}	Tension	4.62, GPa
ν_{12}	Tension	0.39

Table 2 Summary of fracture properties

G_{IC}	472, J/m^2 (Ref. 11)
G_{IIC}	472, J/m^2 (Ref. 11)
G_{IId}	402, J/m^2

Low-Velocity Impact

Beam Specimens

Test Procedure

Five beam specimens with 2.54×6.35 cm (1×2.5 in.) and $[0]_{16}$ layup were used to investigate the effect of loading rate (700 kN/s) on the mode II critical strain-energy release rate. One layer of thin Teflon film 0.50 in. long was inserted at the midplane to introduce a precrack in the laminate. A load cell and a capacitive transducer were used to monitor the load and specimen deflection history, respectively. A 13.5-N cross-head weight was dropped from several heights for this experiment. The threshold impact velocity was 240 cm/s. An oscilloscope was used to record the load and displacement histories during impact.

Finite Element Analysis

A two-dimensional linear finite element analysis was used to model an end-notched flexural specimen (Fig. 13) to calculate the mode II strain-energy release rate variation under low-velocity impact. The discretization used in the final analysis was based on the convergence study of G_{II} as shown in Fig. 14. The model contained 112 isoparametric quadrilateral plane strain elements and had 350 degrees of freedom. The finite element mesh in the vicinity of the crack tip is shown in Fig. 1b where the elements are 0.019×0.0508 cm (0.0075×0.02 in.), which results in an incremental crack extension of $da/a = 0.016$. Gap elements were used between the coincident nodes in the delamination area to prevent overlapping of the material.

The transient dynamic response of the specimen was obtained using the ABAQUS finite element program. This solution sequence employs a direct time integration scheme based on the Newmark method.[12] A time step of 0.01 ms was used in the dynamic analysis of the specimen. In the present analysis, the impact force history, which was recorded directly by a load transducer, was input to the finite element analysis. The dynamic strain-energy release rate G_{IId} was calculated at the maximum load recorded during impact.

Results and Discussion

The force and resultant strain-energy release rate histories are shown in Fig. 15. The dynamic delamination growth seemed to occur at the maximum load level recorded during impact. Table 2 shows the critical strain-energy release rates for mode I, mode II, and dynamic mode II fracture.

Plate Specimens

Test Procedures

Eight panels of 7.62 by 7.62 cm (3×3 in.) and $[(0)_4/(90)_4]_s$ layup were used for this experiment. All specimens were tested in the drop-weight impact test fixture at an impact energy of 1.1 J. The impactor head was 5.78 N (1.3 lb) in weight, and 0.635 cm (0.25 in.) in diameter. The impacted panels were ultrasonic C-scanned to locate and measure the damage area. The impacted panels were also cross sectioned by diamond saw to view the damage distribution and to measure the delamination length through the thickness under a microscope. These damage areas were compared with the damage areas generated in quasistatic tests to correlate the quasistatic and the low-velocity impact test results.

Test Results

The threshold velocity was found to be 185 cm/s (73 in./s). The cross section of impacted specimens shows that the dam-

age area was dominated by the delamination between 0- and 90-deg plies. Similar damage distribution was observed in quasistatic loading of the laminate. Therefore, the finite element approach that was used for quasistatic loading to predict damage area can be used to model low-velocity impact.

Conclusions

A numerical procedure was developed to estimate the delamination area in a graphite/epoxy $[(0)_4/(90)_4]_s$ laminated plate subjected to low-velocity impact. Finite element analysis coupled with either crack closure integral or the change in potential energy for two crack lengths was used to calculate G_{II}. This study resulted in following conclusions:

1) Quasistatic analysis can be used to model the response of composite beams and plates subjected to low-velocity impact.

2) Mode II is the dominant failure mode of delamination propagation. The contribution of G_I to delamination propagation is negligible.

3) Strain-energy release rate is a valid criteria for predicting the delamination area. The criteria for the delamination propagation is $G_{II} \geq G_{IIC}$ and for arrest $G_{II} \leq G_{IIa}$.

4) The dynamic initiations strain-energy release rate under rapid loading G_{IId} is approximately 15% lower than G_{IIC}.

5) The arrest strain-energy release rate G_{IIa} is approximately 75% lower than G_{IIC}.

Acknowledgment

The authors wish to express their gratitude to The Boeing Defense and Aerospace Group for providing the fellowship for this research.

References

[1]Graves, J. M., and Kantz, J. S., "Initiation and Extent of Impact Damage in Graphite/Epoxy and Graphite/Peak Composites," *Proceedings of the AIAA/ASME/ASCE/AHS 29th Structures, Structural Dynamics, and Materials Conference,* AIAA, Washington, DC, April 1988, pp. 967–976 (AIAA Paper 88-2327).

[2]Clark, G., "Modeling of Impact Damage in Composite Laminate," *Composites,* Vol. 20, No. 3, 1989, pp. 209–214.

[3]Bostaph, G. M., and Elber, W., "A Fracture Mechanics Analysis for Delamination Growth During Impact on Composite Plates," *Advances in Aerospace Structures, Materials, and Dynamics,* American Society of Mechanical Engineers, New York, 1983, pp. 133–138.

[4]Grady, J. E., and Sun, C. T., "Dynamic Delamination Crack Propagation in a Graphite/Epoxy Laminate," *Composite Materials: Fatigue and Fracture, ASTM STP 907,* edited by H. T. Hahn, American Society for Testing and Materials, Philadelphia, PA, 1986, pp. 5–31.

[5]Grady, J. E., and Depaola, K. J., "Measurement of Impact-Induced Delamination Buckling in Composite Laminates," *Dynamic Failure; Proceedings of the 1987 SEM Fall,* Society for Experimental Mechanics, Bethel, CT, 1987, pp. 250–255.

[6]Gosse, J. H., and Mori, P. B. Y., "Impact Damage Characterization of Graphite/Epoxy Laminates," *Proceedings of the American Society for Composites,* 3rd Technical Conference on Composite Materials, American Society for Composites, Seattle, WA, 1988, pp. 187–193.

[7]Gosse, J. H., Mori, P. B. Y., and Avery, W. B., "The Relationship Between Impact-Induced Stress States and Damage Initiation and Growth in Composite Plates," *Materials—Processes: The Intercept Point,* Society for the Advancement of Materials and Process Engineering, Seattle, WA, 1988, pp. 187–193.

[8]Choi, H. Y., Wu, H. T., and Chang, F. K., "A New Approach Toward Understanding Damage Mechanism and Mechanics of Laminated Composites Due to Low-Velocity Impact, Part I—Experiments," *Journal of Composite Materials,* Vol. 25, Aug. 1991, pp. 992–1011.

[9]Finn, S., "Delaminations in Composite Plates Under Transverse Static or Impact Loading," Ph.D. Dissertation, Dept. of Mechanical Engineering, Stanford Univ., Stanford, CA, 1991.

[10]Rybicki, E. F., and Kanninen, M. F., "A Finite Element Calculation of Stress Intensity Factors by a Modified Crack Closure Integral," *Engineering Fracture Mechanics,* Vol. 9, No. 4, 1977, pp. 931–938.

[11]Razi, H., "An Experimental and Numerical Study of Delamination Propagation and Arrest in Composite Beams and Plates When Subjected to Low-Velocity Impact," Ph.D. Dissertation, Dept. of Mechanical Engineering, Univ. of Washington, Seattle, WA, 1991.

[12]Newmark, N. M., "A Method of Computation for Structural Dynamics," *Journal of the Engineering Mechanics Division in Proceedings of American Society of Civil Engineering,* American Society of Civil Engineering, Ann Arbor, MI, Vol. 85, July 1959, p. 67.